Desalination and Water Treatment
www.deswater.com
doi: 10.5004/dwt.2023.30002

312 (2023) 1–13
November

Influence of *in-situ* NaClO backwashing on the biological performance and membrane fouling behavior in a granule-based SNAD-MBR process

Zhaozhao Wang[a,b], Dameng Lian[a,b], Shuhao Zhu[a,b], Lina Yan[c], Simin Li[a,b,*]

[a]*College of Energy and Environmental Engineering, Hebei University of Engineering, Handan 056038, China*
[b]*Center for Water Pollution Control and Water Ecological Remediation, Hebei University of Engineering, Handan 056038, China, Tel.: +8617831917609; email: a17831917609@163.com (S.M. Li), W-Z-Z@163.com (Z.Z. Wang), liandameng@163.com (D.M. Lian), ZSH19981015@163.com (S.H. Zhu)*
[c]*College of Environmental and Energy Engineering, Beijing University of Technology, Beijing 100124, China, email: yanlina01@126.com*

Received 10 June 2023; Accepted 26 September 2023

ABSTRACT

A granule-based simultaneous nitrification, anammox, and denitrification process in a membrane bioreactor (SNAD-MBR) was performed to investigate the influence of *in-situ* NaClO backwashing on biological performance and membrane fouling. First, the limit of the NaClO concentration for the SNAD granules was determined (20 mg/g·SS) in a short-term batch test. Then, three *in-situ* NaClO backwashing strategies (NaClO concentrations of 5–15 mg/g·SS with backwashing frequencies of 1/10–1/30 min) were implemented during long-term SNAD-MBR process. The results showed that the removal efficiencies of total nitrogen (TN) and chemical oxygen demand decreased from 92.69% and 94.19% to 81.82% and 85.39%, respectively, with an increase in the NaClO concentration in spite of a reduction in backwashing frequency. The deterioration of the biological performance could be explained by the inhibitory activities of the functional bacteria after long-term exposure to NaClO. Nevertheless, the stable contributions of autotrophic and heterotrophic processes to TN removal ($E_{anammox}$ of 91.23%, $E_{denitrification}$ of 8.77%) indicated a negligible impact of NaClO backwashing on the balance of the nitrogen removal pathways. Furthermore, membrane fouling was significantly suppressed when *in-situ* NaClO backwashing was performed with a relatively high frequency (1/1–10/20min) and a low concentration (5–10 mg/g·SS). However, a higher NaClO concentration (15 mg/g·SS) exacerbated membrane fouling, although the backwashing frequency was low. Meanwhile, the high fouling potential of the SNAD granules resulted from the high production of soluble microbial products (especially tryptophan protein-like substances) under NaClO stress. The possible underlying mechanism was the trade-off between the membrane scrubbing effect by NaClO and the variable physico-chemical properties of the SNAD granules. The optimal *in-situ* NaClO backwashing strategy that considered the process performance, membrane fouling, and permeate production was a NaClO concentration of 15 mg/g·SS and a backwashing frequency of 1/20 min. The results provide guidance for *in-situ* NaClO backwashing of the SNAD-MBR process.

Keywords: Simultaneous nitrification, anammox and denitrification (SNAD); Membrane bioreactor; Membrane fouling; NaClO backwashing; Chemical cleaning

* Corresponding author.

1. Introduction

Excessive nitrogen discharge can trigger the eutrophication of water bodies, posing a serious threat to water safety and human health. Several biological nitrogen removal processes have been developed to achieve high-efficiency nitrogen removal. Anaerobic ammonia oxidation (anammox) is considered the most cost-effective and sustainable biological process. In this process, a class of *Planctomycetes* converts the ammonia nitrogen and nitrite substrates into dinitrogen under anaerobic conditions, resulting in a total nitrogen (TN) removal efficiency of 90% with a relatively low sludge yield rate. Sewage (e.g., urban wastewater) contains ammonia and organic matter as the main contaminants. Therefore, nitritation is essential to provide substrates (NO_2^-–N) for anaerobic ammonia oxidation. Moreover, denitrification is required to reduce the inhibitory activities of anaerobic ammonium-oxidizing bacteria (AnAOB) and remove nitrate from the anammox process to improve the TN removal efficiency. Therefore, the simultaneous nitrification, anammox and denitrification (SNAD) process was developed and has been used for urban sewage treatment [1].

Anammox is the core reaction in the SNAD process, and the effective retention of AnAOB is critical to ensure the efficient operation of the SNAD process. A membrane bioreactor (MBR) is frequently employed as a valid alternative to enhance AnAOB retention and has stable biological nitrogen removal efficacy. Li et al. [2] reported that the high retention efficiency of AnAOB enabled a stable N removal efficiency of 98.35% in an anammox process in an MBR. Zhao et al. [3] demonstrated the excellent performance of an MBR for rapid start-up and stable biological performance of the SNAD process. However, membrane fouling remains a problem in the SNAD-MBR process, limiting its application scope.

In-situ maintenance cleaning is an effective strategy for suppressing membrane fouling and achieving the sustainable operation of the MBR process. *In-situ* maintenance cleaning can be categorized into hydraulic and chemical backwashing. Hydraulic backwashing removes membrane foulants (i.e., part of the cake layer) caused by physical interactions with the membranes. Chemical backwashing is a supplement to hydraulic backwashing and removes foulants by chemical interactions (i.e., membrane pore blocking), restoring permeability and permeate production. NaClO is a commonly used chemical reagent, and the concentration and backwashing frequency of NaClO are critical for the sustainable operation of the MBR process [4]. Scholars have reported the effects of different NaClO concentrations on microbial activities and sludge fouling potential using sequencing batch tests [5–7]. Han et al. [5,6] investigated the stress effect of microorganisms in an aerobic MBR in the presence of NaClO in static experiments. The results showed that NaClO at concentrations higher than 1 mg/g·SS disrupted the integrity of microbial cells, inhibited cell metabolic activities, and promoted polysaccharide oxidation, amino acid deformation, and the destruction of protein secondary structures in extracellular polymeric substances (EPS). These effects could reduce the treatment efficacy and exacerbate membrane fouling of the MBR process. Cai and Liu [7] evaluated the effect of NaClO on membrane fouling using sequential batch cross-flow filtration tests and aerobic sludge. The results suggested the membrane fouling rate was significantly increased when the NaClO concentration was 20 mg/L. This result was attributed to the increased EPS production by accelerated bacterial dissolution, causing the residual bacteria to adhere to the membrane surface under higher NaClO stress.

In addition, studies have been conducted on maintaining membrane permeability by periodic NaClO backwashing. Yue et al. [8] investigated the influence of the NaClO concentration during chemical backwashing on the performance of a continuous-flow anaerobic ceramic MBR process. A NaClO concentration of 1 mg/L prevented membrane fouling and provided the optimum process performance of the system. Wang et al. [9] proposed a maintenance cleaning strategy of reducing the NaClO concentration and increasing the backwashing frequency. This approach significantly suppressed membrane fouling and extended the operating cycle of the MBR process. Jiang et al. [10] investigated the effect of NaClO on membrane fouling of a continuous-flow anammox process in a MBR process. The results indicated that NaClO could oxidize the carbohydrate-like components in the membrane pores. The optimum cleaning strategy consisted of a NaClO concentration of 298 mg/L and a backwashing duration of 15 min.

These studies indicate that an appropriate *in-situ* NaClO backwashing strategy can inhibit membrane fouling and maintain membrane permeability. However, unlike in an aerobic process, the functional microflora is diverse, and the sludge properties are variable in the SNAD process. Hence, the influence mechanisms of online chemical backwashing on the SNAD-MBR process remain unclear. The optimization of *in-situ* NaClO backwashing strategies is required to extend the operating cycle of the system and minimize adverse impacts on the activities of functional microorganisms.

Accordingly, the tolerance limits of different functional bacteria to the NaClO concentration were determined by sequencing batch tests. The effects of periodic NaClO backwashing with different concentrations and frequencies on the nitrogen and carbon removal efficacies and membrane fouling in the SNAD-MBR process were investigated. Moreover, the effect of NaClO on the system was analyzed by investigating changes in the activities of functional bacteria and the physico-chemical/biochemical properties of the SNAD granules during a long-term operation. The *in-situ* NaClO backwashing strategy was optimized, providing theoretical guidance and support for the sustainable operation of the SNAD-MBR process.

2. Materials and methods

2.1. Experimental set-up and operation

The up-flow microaerobic sludge blanket (UMSB) reactor consisted of a sleeve-shaped plexiglass material with an effective volume of 4.5 L (Fig. 1). The outside of the reactor was covered with black material to preserve heat and block the light. A circulating water bath with two heating rods submerged in the circulation tank was used to ensure that the temperature of the main reactor was constant. The reactor was equipped with an external reflux pump, and the velocity was controlled by adjusting the speed of the reflux

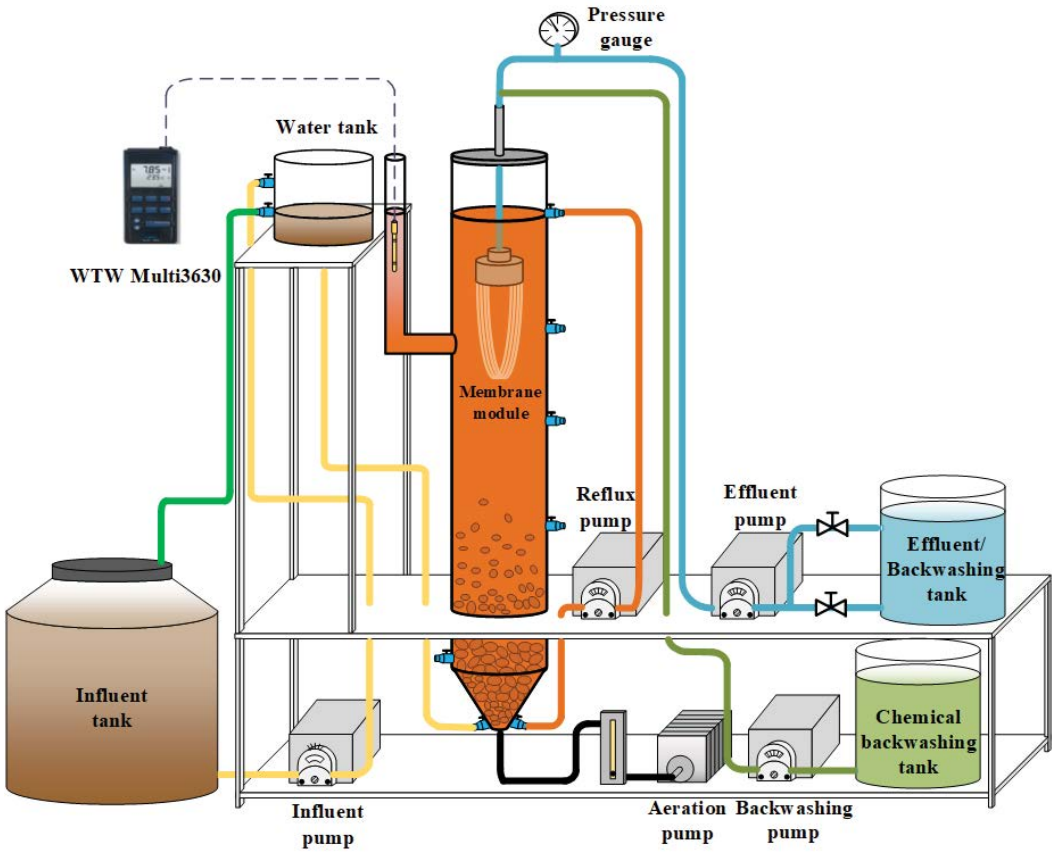

Fig. 1. Schematic diagram of the UMSB-MBR reactor.

pump. The synthetic wastewater and the reflux flow entered the bottom of the reactor, and the effluent was pumped out through the membrane module to the water tank.

A hollow fiber membrane module (pore size, 0.3 μm, surface area, 0.075 m^2, consisting of polyvinylidene fluoride and obtained from Hangzhou Mina Membrane Technology Corporation, China) was operated at a constant flux (~6.7 L/(m^2·h)) with intermittent suction (9.0-min suction and 1.0 min rest) in phase I. Chemical backwashing was employed in phase II, with a cleaning cycle of 10 min, including 8 min for water production, 1 min for hydraulic backwashing, and 1 min for chemical backwashing. The cleaning cycle of phase III was 20 min; the first 10 min was the same as that of phase I, and the subsequent 10 min was the same as that of phase II. The cleaning cycle in phase IV lasted 30 min; the first 20 min was the same as that of phase I, and the subsequent 10 min was the same as that of phase II. At the end of each phase, the fouled membrane module was removed from the reactor for foulant extraction, and a new membrane module was installed for the subsequent operational phase.

The transmembrane pressure (TMP) was monitored by a pressure gauge. A microporous aeration disc was installed at the bottom of the reactor and was connected to an air compressor to supply dissolved oxygen (DO) to the reactor. A pH-DO sensor (Multi 340i, WTW Corporation, Germany) was used to monitor the DO and pH levels in the reactor. A circulating water bath system was used to maintain the temperature at 30°C ± 2.0°C.

2.2. Inoculated sludge and synthetic wastewater

2.2.1. Inoculated sludge and process performance

The inoculated sludge (SNAD granules) was obtained from a pilot-scale UMSB-MBR used for the treatment of low C/N ratio synthetic wastewater. Synthetic sewage was used as the substrate for the pilot-scale UMSB-MBR, and the nitrate and organic matter originated from NH_4Cl and sodium acetate, respectively. The average concentrations of NH_4^+–N and chemical oxygen demand (COD) in the feed were maintained at 50 and 50 mg/L, with removal efficiencies of 97.5% and 92.3%, respectively.

2.2.2. Synthetic wastewater

Synthetic wastewater was used as the substrate in this study; the ammonia and organic matter originated from NH_4Cl and sodium acetate, respectively. The concentrations of nitrogen and organic matter differed for different experimental groups (Table 1). The C/N ratio was maintained at approximately 1.0, which referred to the optimal influent parameter for the SNAD-MBR in our previous study. The other components and trace elements in the synthetic wastewater were as follows: 500 mg/L $NaHCO_3$; 27.2 mg/L KH_2PO_4; 180 mg/L $CaCl_2{\cdot}2H_2O$; 300 mg/L $MgSO_4{\cdot}7H_2O$. Trace elements I and II were supplied at 1 mL/L. The composition of trace element I was 1.25 g/L $KHCO_3$, 0.025 g/L KH_2PO_4, 0.3 g/L $CaCl_2{\cdot}2H_2O$, 0.2 g/L $MgSO_4{\cdot}7H_2O$, and 0.00625 g/L

Table 1
Operational conditions and substrates of the SNAD-MBR process

Phase	Operation time (d)	NH_4^+–N (mg/L)	Chemical oxygen demand (mg/L)	Backwashing flux (LMH)	Backwashing frequency (min/min)	NaClO concentration (mg·NaClO/g·MLSS)
I	1–14	51.67 ± 0.90	50.34 ± 0.28	20.1	0/0	0
II	15–44	51.59 ± 0.49	52.08 ± 1.61	20.1	1/10	5
III	45–74	51.06 ± 0.92	52.61 ± 1.94	20.1	1/20	10
IV	75–105	51.51 ± 1.20	52.67 ± 1.19	20.1	1/30	15

$FeSO_4$, and that of trace element II was 15 g/L EDTA, 0.43 g/L $ZnSO_4·7H_2O$, 0.24 g/L $CoCl_2·6H_2O$, 0.99 g/L $MnCl_2·4H_2O$, 0.25 g/L $CuSO_4·5H_2O$, 0.22 g/L $NaMoO_4·2H_2O$, 0.19 g/L $NiCl_2·6H_2O$, 0.21 g/L $NaSeO_4·10H_2O$, 0.014 g/L H_3BO_3, and 0.05 g/L $Na_2WO_4·2H_2O$.

2.3. Sample analyses and methods

The contents of COD, NH_4^+–N, NO_2^-–N, NO_3^-–N, mixed liquor suspended solids (MLSS), and mixed liquor volatile suspended solids (MLVSS) were measured according to standard methods [11], and the TN concentration was the sum of the NH_4^+–N, NO_2^-–N, and NO_3^-–N concentrations. The particle size distribution of the granular sludge was determined by wet-sieving using stainless steel sieves with aperture diameters of 3.0, 2.5, 2.0, 1.5, and 1.0 mm.

The concentration of EPS was determined by measuring the amount of protein and carbohydrates using a heating extraction method [12]. The protein fraction of EPS (EPS_p) and the carbohydrate fraction of EPS (EPS_c) were determined using the modified Bradford method with bovine serum albumin as the standard and the anthrone-sulfuric acid colorimetric method with glucose as the standard [13], respectively.

The three-dimensional excitation-emission matrix (3D-EEM) spectra of the EPS and soluble microbial products (SMP) were obtained using a fluorescence spectrometer (Hitachi F-7100, Tokyo, Japan). The excitation and emission slits were maintained at 10 nm, and the scanning speed was 60,000 nm/min. The EEM spectra were collected at excitation wavelengths from 200 to 550 nm at 10 nm increments. The data were processed and analyzed using Origin 8.5 Software (OriginLab Northampton, MA, USA).

2.4. Analysis of the activities of the functional bacteria

Sequencing batch tests were parallelly conducted with 250 mL serum flasks for 7 h. The granular sludge was obtained from the bottom of the SNAD-MBR at the end of each operational phase and was cleaned with distilled water three times to remove the remaining matrix on the sludge surface. About 12 g of wet granular sludge was added to the serum bottles containing the substrates, as shown in Table 2. The NH_4^+–N, NO_2^-–N, and NO_3^-–N concentrations in the supernatants of the serum flasks were determined once in an hour. The activities of aerobic ammonium-oxidizing bacteria (AerAOB), anaerobic ammonium-oxidizing bacteria (AnAOB), and denitrifying bacteria (DNB_a and DNB_b) were characterized by evaluating the NH_4^+–N, TN, NO_2^-–N, and NO_3^-–N specific degradation rates (mg·N/mg·MLVSS·d), respectively.

Table 2
Substrates of the sequencing batch tests

Functional bacteria	NH_4^+–N (mg/L)	NO_2^-–N (mg/L)	NO_3^-–N (mg/L)	Chemical oxygen demand (mg/L)
AerAOB	50	0	0	0
AnAOB	25	33	0	0
DNB_a	0	30	0	50
DNB_b	0	0	20	50

The inhibition degree of the microbial activity is denoted as R in Eq. (1).

$$R = \frac{S_e}{S_0} \times 100\% \tag{1}$$

where R is the inhibition degree, (%); S_e is the decrease in the microbial activity under NaClO stress (mg·N/mg·MLVSS·d), and S_0 is the initial microbial activity without NaClO stress (mg·N/mg·MLVSS·d).

2.5. Evaluation of membrane fouling behavior

2.5.1. Calculation of membrane fouling rate

The TMP (kPa) data were corrected using the standard temperature (T, 20°C) [14], as defined in Eq. (2):

$$\mathrm{TMP} = \mathrm{TMP}_\theta e^{0.023(\theta-20)} \tag{2}$$

The membrane fouling rate was determined with Eq. (3):

$$F_r = \frac{\Delta \mathrm{TMP}}{\Delta t} \times 100\% \tag{3}$$

where F_r is the membrane fouling rate (Pa/h), TMP is the transmembrane pressure (kPa), and t is the running time (h).

2.5.2. Membrane foulant extraction

At the end of each phase, the filter cake layer on the surface of the contaminated membrane was gently wiped with a sponge, and the fouled membrane module was immersed in a NaOH solution with a pH of 12 and placed at 30°C for 24 h. Approximately 100 mL of the solution was filtered

through a 0.45 μm membrane and placed in a dryer at 105°C for 24 h to obtain the dry foulants.

2.5.3. Fourier-transform infrared spectroscopy and protein secondary structure analysis

The dry foulants were mixed with KBr in an agate grinder at the ratio of 1:100. The mixture was compressed, and the main functional groups in the membrane foulants were analyzed by Fourier-transform infrared spectroscopy (FT-IR) (IRAffinity-1, Japan) at 4,000–400 cm^{-1}. Self-deconvolution was used in the amide I region of 1,700–1,600 cm^{-1} [15]. The PeakFit software (version 4.12) was used to calculate the second-derivative spectrum and fitting curve to analyze the protein secondary structure.

2.6. Redundancy analysis

Canoco 5 (v.5.15, Microcomputer power, USA) software was used for redundancy analysis of the experimental data. The cosine of the angle between the arrows represents the degree of correlation between the variables. The larger the cosine value, the greater the correlation; the arrow direction represents positive (same direction) or negative (different directions) correlations. A vertical arrow indicates no correlation.

3. Results and discussion

3.1. Influence of NaClO on biological performance of the SNAD-MBR process

3.1.1. Short-term influence of NaClO on the activities of functional bacteria

The SNAD granules formed during the start-up period of the SNAD process (this period is not shown). Granular sludge typically has larger biomass than activated flocs, resulting in higher activities of the degrading substrates [16]. The SNAD granules achieve advanced nitrogen removal due to the synergy of multiple types of functional bacteria (AerAOB, AnAOB, and DNB) that utilize autotrophic and heterotrophic pathways [17]. The activities of the functional bacteria under different levels of NaClO stresses (0–40 mg/g·MLSS) were investigated by batch tests to determine the limit of the NaClO concentration. AerAOB prefer to remain on the surface of SNAD granules due to the oxygen demand, whereas AnAOB prefer anaerobic conditions and are found in the interior of the granules to achieve ammonia and nitrite removal. The distribution of DNB is more complex; they exist on the surface or the interior of the granules because some favor an anoxic environment.

Fig. 2 shows that the activities of AerAOB, AnAOB, DNB_a, and DNB_b were 0.4305, 0.477, 0.35, and 0.224 mg·N/(mg·VSS·d) without NaClO stress, respectively. In comparison, a previous study presented lower activities of AerAOB, AnAOB, DNB_a, and DNB_b for 0.216, 0.323, 0.072, and 0.196 mg·N/(mg·VSS·d), respectively, in a SNAD system treating synthetic municipal wastewater [1]. The discrepancies were possibly attributed to the different influent C/N ratio, which could exhibit significant impacts on abundance of functional bacteria. The activities of the functional bacteria at NaClO concentrations of 10 and 20 mg/g·MLSS showed no significant differences (ANOVA, $p < 0.05$), which were slightly inhibited with R values of 96.40, 97.48, 96.57, and 95.98 and 92.92, 93.29, 93.71, and 91.52 for AerAOB, AnAOB, DNB_a, and DNB_b, respectively, indicating similar inhibition degrees for all functional bacteria.

Nevertheless, significant inhibitions of the activities of functional bacteria were observed at higher NaClO concentrations of 30 and 40 mg/L, with R values of 74.33, 78.62, 77.14, 75.89, and 58.07, 64.99, 62.86, 62.50 for AerAOB, AnAOB, DNB_a, and DNB_b, respectively. The relatively higher R values for AnAOB and DNB than for AerAOB were attributed to the granular structure, which provided a protective barrier for the cells due to the high microbe density, the EPS matrix, and inorganic salts. Thus, the bacteria exhibited high resistance to toxic compounds [18]. Notably, the granular sludge readily disintegrated when exposed to high stress. Therefore, it is critical to obtain the limit of the NaClO concentration to implement periodic backwashing during the long-term operation of the SNAD-MBR process.

The results indicated that the limit of the NaClO concentration was 20 mg/g·MLSS for the SNAD granules. Three NaClO concentrations (not exceeding 20 mg/g·MLSS) and different backwashing frequencies were tested to investigate the long-term influence of NaClO on the process performance.

3.1.2. Long-term influence of NaClO on biological performance

The nitrogen and organic contaminant removal performances of the SNAD-MBR process with periodic NaClO backwashing are shown in Fig. 3a and b. In phase I, high nitrogen and organic contaminant removal efficiencies were achieved by coupling anammox and denitrification with an ammonia removal efficiency (ARE) of 97.34%, nitrogen removal efficiency (NRE) of 93.31%, and COD removal efficiency (CRE) of 93.17%. The favorable performance was closely related to the high activities of the functional bacteria.

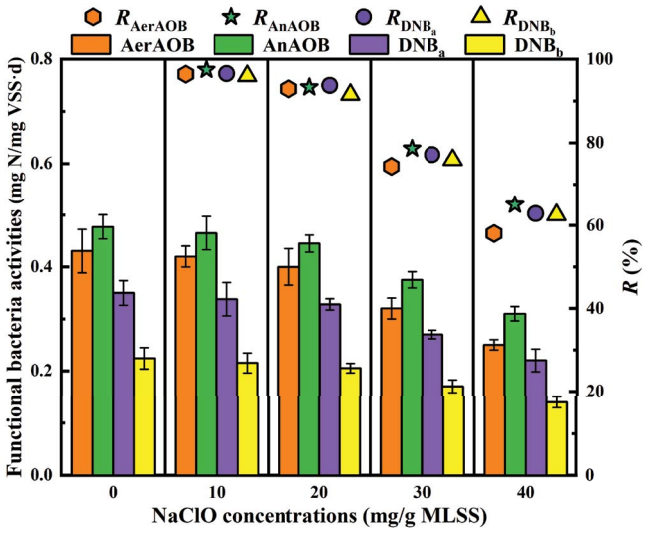

Fig. 2. Activities of functional bacteria at different NaClO concentration.

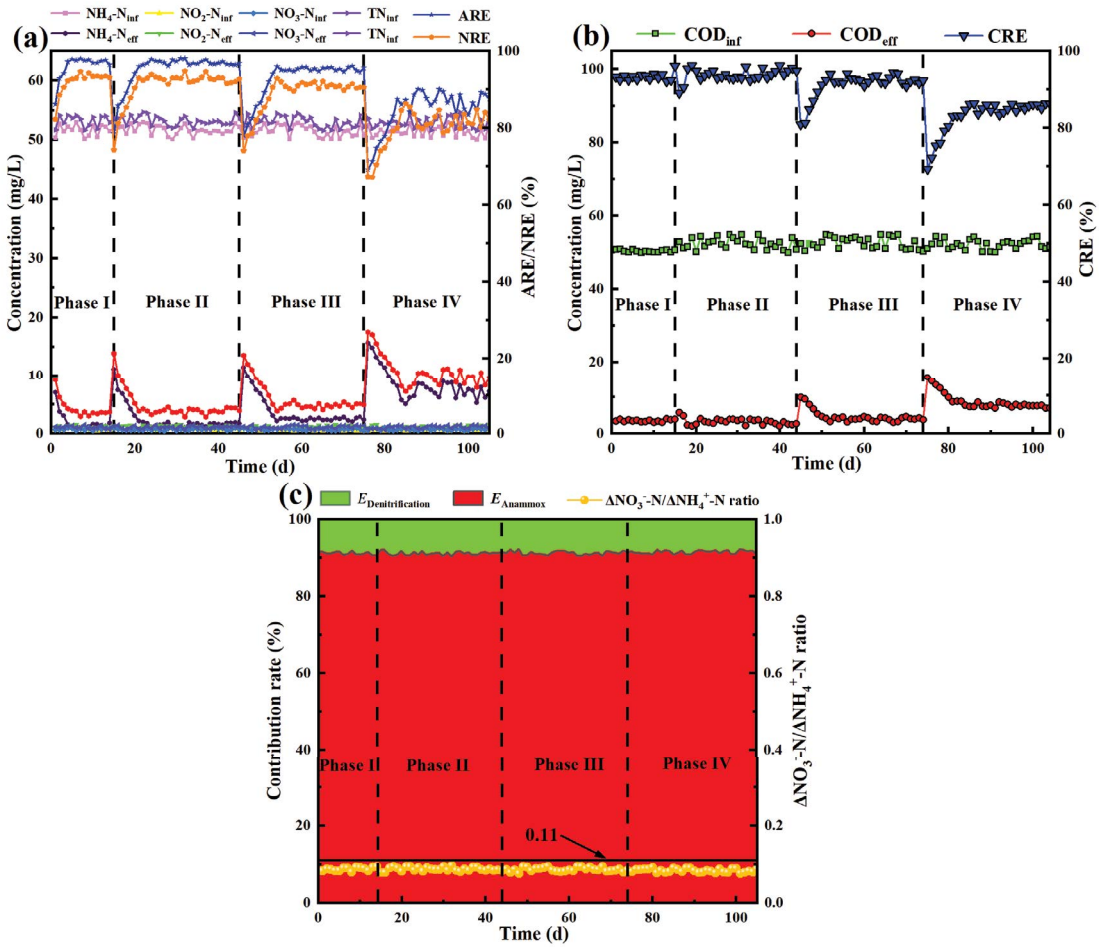

Fig. 3. Performance of SNAD-MBR during different operational phases. (a) Nitrogen removal, (b) chemical oxygen demand removal and (c) changes in contribution rate of anammox and denitrification pathways.

Table 3
Activities of functional bacteria during different operational phases

Phase	AerAOB (mg·N/(mg·MLVSS·d))	AnAOB (mg·N/(mg·MLVSS·d))	DNB_a (mg·N/(mg·MLVSS·d))	DNB_b (mg·N/(mg·MLVSS·d))
I	0.4305 ± 0.042	0.477 ± 0.023	0.35 ± 0.024	0.224 ± 0.021
II	0.41 ± 0.031	0.455 ± 0.032	0.33 ± 0.012	0.213 ± 0.014
III	0.38 ± 0.025	0.425 ± 0.027	0.305 ± 0.22	0.198 ± 0.018
IV	0.28 ± 0.018	0.315 ± 0.015	0.22 ± 0.021	0.15 ± 0.017

As shown in Table 3, the activities of AerAOB, AnAOB, DNB_a, and DNB_b were 0.4305, 0.477, 0.35, and 0.224 mg·N/(mg·MLSS·d), respectively. Periodic NaClO backwashing had a negligible impact on the biological performance, with ARE and NRE of 96.81% and 92.69%, respectively, a NaClO concentration of 5 mg/g·SS, and a backwashing frequency of 1/10 min. Minor reductions in the activities of functional bacteria (0.41, 0.455, 0.33, and 0.213 for AerAOB, AnAOB, DNB_a, and DNB_b) were also observed, explaining the performance variation. As the NaClO concentration increased, the nitrogen and organic contaminant removal efficiencies increased, although the backwashing frequency was lower. Similar trends were discovered in the activities of AerAOB, AnAOB, and DNB. The ARE, NRE, and CRE decreased to 86.56%, 81.82%, and 85.39%, and the activities of AerAOB, AnAOB, DNB_a, and DNB_b remained low at 0.28, 0.315, 0.22, and 0.15 mg/g·MLSS, respectively. The NaClO concentration used during periodic backwashing was below the limit derived from the sequencing batch tests. However, detrimental influences on the biological performance due to the NaClO concentration were observed due to the periodic shock during the long-term operation. The higher production of intracellular reactive oxygen species (ROS) under higher NaClO stress could damage the cell structure, inhibit key

biodegradation enzymes, and reduce the metabolic activities of microorganisms [5]. These results demonstrate that a periodic NaClO shock with a high concentration and low frequency resulted in greater inhibitory microbial activities, whereas NaClO backwashing with low concentrations and a high frequency was more beneficial for biological nitrogen and carbon removals, although the total same amount of NaClO entered the SNAD-MBR system in one day (0.36 g/d).

In addition, the inhibition degrees of the activities of different functional bacteria were similar under periodic NaClO shock. In the sequencing batch test, the inhibition degree of AerAOB was higher under NaClO stress, whereas AnAOB and DNB were more adaptable to unfavorable environments because they prefer anaerobic conditions inside of the SNAD granules. However, the SNAD granular structure exhibited little resistance to the NaClO shock during the long-term operation. This finding was attributed to the coupling relationships of the three functional bacteria for synergistic nitrogen and carbon removal. After the AerAOB (on the outside of the SNAD granules) were inhibited by NaClO, the AnAOB (on the inside of the granules) were suppressed due to the shortage of substrates produced by the AerAOB (e.g., NO_2^-–N) during the long-term operation. The DNB were also inhibited due to the reduction in NO_3^-–N, which was attributed to the coupling relationship of AerAOB and AnAOB in the completely autotrophic nitrogen removal over nitrite (CANON) process. Moreover, periodic NaClO shocks with higher concentrations caused the disintegration of granular sludge, leading to a reduction in the resistance to unfavorable environments [19].

Therefore, the inhibition degrees of the three types of functional bacteria were likely similar. Anammox was the dominant pathway (91.13%–91.46%), and denitrification was a supplementary pathway during nitrogen removal during different operational phases (8.87%–8.54%). Moreover, the NO_3^-–N/NH_4^+–N ratio was always higher than the theoretical value of 0.11 in the CANON process, indicating a coupling relationship between the three functional bacteria, although the nitrogen and carbon removal efficiencies were lower under NaClO stress.

3.2. Influence of NaClO on membrane fouling in the SNAD-MBR process

3.2.1. Influence of NaClO on membrane fouling rate and permeate production

The membrane fouling rate and permeate production during different operational phases are shown in Fig. 4. The SNAD-MBR process was operated at a constant flux (6.6–6.9 LMH), and the TMP increased with the operational time, regardless of the chemical backwashing. The membrane fouling rate was attributed to two factors: dislodging of the membrane foulants and the change in the properties of the mixed liquor [4].

The fouling rate in the SNAD-MBR process was relatively higher (3.89 Pa/h) in phase I without physical or chemical backwashing. The permeate production remained close to 10.7 L/d. In contrast, membrane fouling was significantly suppressed in phase II, with a lower fouling rate of 0.97 Pa/h. The physical cleaning (permeate backwashing) could restore membrane permeability by dislodging the easily detached foulants on the membrane surface (e.g., part of the cake layer). However, only chemical backwashing could remove membrane foulants that caused deep pore blocking. Thus, it was inferred that the scrubbing of NaClO backwashing was the most effective at a low NaClO concentration of 5 mg/g·SS. However, the permeate production decreased to 9.69 L/d due to the high backwashing frequency of 1/10 min.

The fouling rate was 2.66 Pa/h in phase III, lower than that of phase I but higher than that of phase II. A higher NaClO concentration with a lower frequency (10 mg/g·SS, 1/20 min) substantially suppressed membrane fouling, although the fouling potential of the SNAD granules was enhanced. The permeate production was improved (average 10.36 L/d) due to the lower backwashing frequency. In contrast, a higher fouling rate (7.58 Pa/h) was observed in phase IV. These results demonstrated that periodic chemical cleaning for permeability maintenance with a higher NaClO concentration (15 g/g·SS) and a lower frequency (1/30 min) was unsuitable. The possible reason was the deteriorated filterability of the SNAD granules due to the variability in the sludge properties (e.g., particle size, SMP, and EPS). The high permeate production (10.52 L/d) did not compensate for this shortcoming because a long-term sustainable operation was impossible for this cleaning protocol.

In summary, the NaClO backwashing protocol substantially affected membrane fouling and permeate production. A lower NaClO concentration and a higher frequency proved optimal for the permeability maintenance in the SNAD-MBR process due to sufficient cleaning performance by NaClO based on the fouling potential of the SNAD granules caused by its physico-chemical properties.

3.2.2. Influence of NaClO on membrane foulants

The foulants on the membrane surface and in the membrane pores resulted from the accumulation of the mixed liquor after the detachment of foulants by NaClO backwashing. Notably, the cake layer was negligible in the

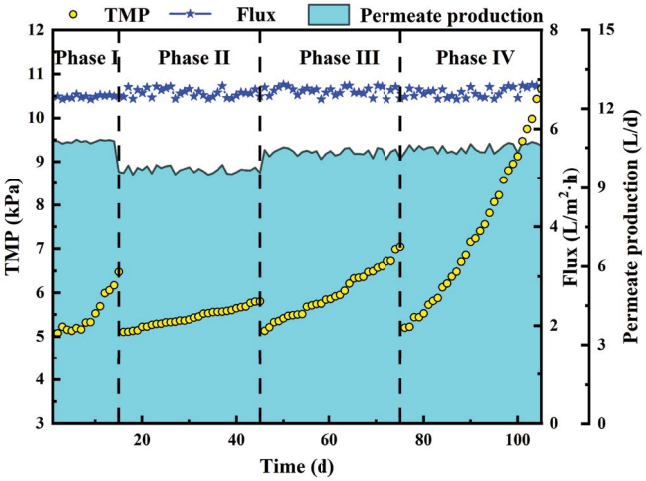

Fig. 4. Changes of membrane fouling behavior and permeate production during different operational phases.

MBR process, whereas deep pore blocking was dominant [20]. Thus, SMPs were primarily responsible for membrane fouling. The types and relative contents of the functional groups of the membrane foulants were analyzed by FT-IR spectroscopy (Fig. 5). Similar spectral profiles were observed for the membrane foulants, suggesting that the compositions of the membrane foulants did not significantly differ during different operational phases. The mechanisms of NaClO scrubbing with different NaClO concentrations and frequencies and the accumulation of SMP in the membrane pores exhibited negligible differences. The proteins and carbohydrates were oxidized, and soluble organic matter originated from the SNAD granules under NaClO stress [10]. The broad adsorption peak at 3,430 cm^{-1} was assigned to the O–H stretching vibrations in the hydroxyl functional groups, and a slight peak at 2,930 cm^{-1} was attributed to the C–H expansion vibrations in alkane organic matter [21]. The peaks near 1,654 cm^{-1} were attributed to the stretching vibrations of C=O and N–H and the deformation vibrations of C–H (amide I vibration of the protein-like substances), respectively [22]. The small adsorption peak at 1,087 cm^{-1} originated from the C–O–C stretching vibrations of carbohydrate-like substances [23].

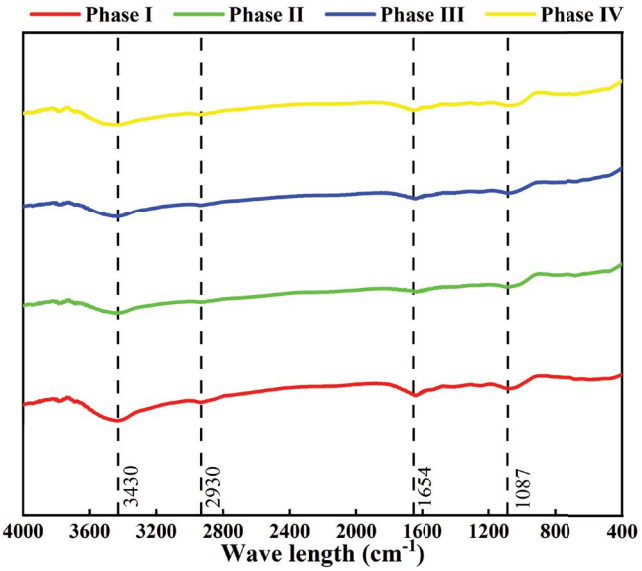

Fig. 5. Infrared spectrum of membrane foulants during different operational phases.

The soluble protein fraction was closely related to the degree of membrane pore blocking [24]. The protein secondary structures of the membrane foulants indicated the inherent interactions between the soluble protein and the membrane. Hence, the amide I region of the infrared spectrum (1,600–1,700 cm^{-1}) of the membrane foulants during different operational phases was analyzed. The differences in the protein secondary structures were determined by second derivative analysis and curve fitting. The fitting results are shown in Fig. 6a–d, and the relative concentrations of the aggregated strands (1,610–1,625 cm^{-1}), α-helices

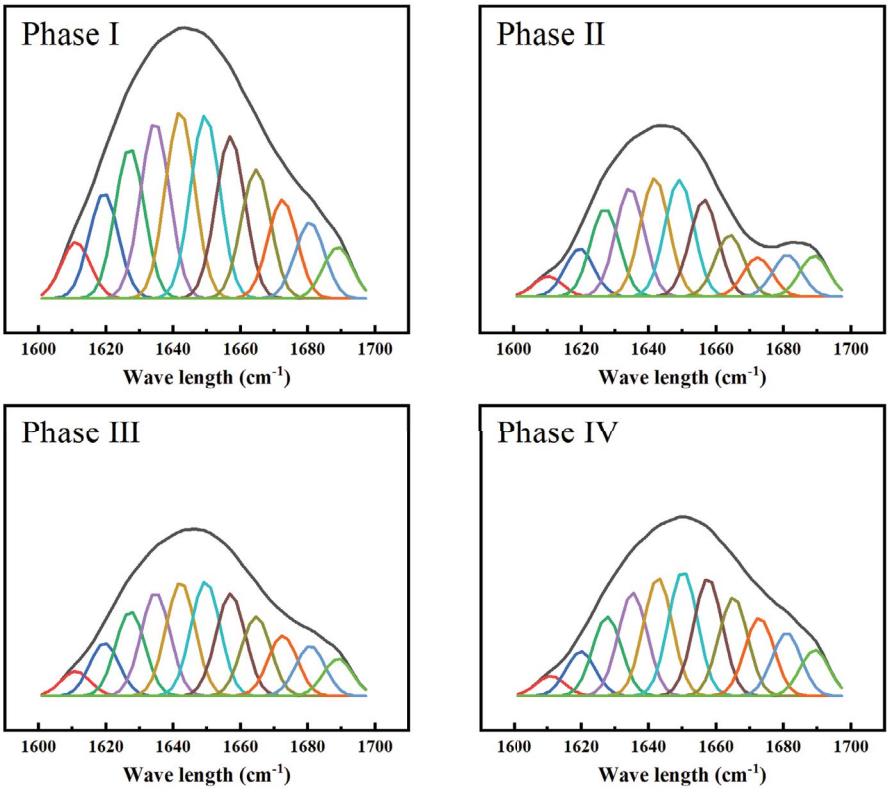

Fig. 6. Infrared spectrum and second-order derivatives of amide I region (1,600~1,700 cm^{-1}) resolution enhancement and curve fitting of membrane foulants substances during different operational phases.

(1,648–1,657 cm^{-1}), β-sheets (1,630–1,640 cm^{-1}), and random coils (1,640–1,645 cm^{-1}) are listed in Table 4. The α-helix fraction (24.48%–27.23%) was higher than the other two fractions (β-sheets: 12.80%–13.69%; random coils: 13.60%–15.26%), indicating that α-helices were dominant in the protein secondary structure. The α-helices/(β-sheets + random coils) ratio indicates the compactness of the protein structure. A low ratio indicates a loose structure and relatively strong hydrophobicity of the protein [25].

The ratio of α-helices/(β-sheets + random coils) decreased from 0.95 to 0.918, suggesting a reduction in the compactness and an increase in the hydrophobicity of the protein in the membrane foulants from phase I to IV. This finding implied that NaClO backwashing with a higher concentration increased the production of hydrophobic soluble proteins, which exhibited stronger interaction forces with the membrane, resulting in irreversible fouling. Thus, these results could explain the higher membrane fouling rate in the SNAD-MBR process in phase III.

3.2.3. Influence of NaClO on sludge properties of SNAD granules

3.2.3.1. Particle size distribution

The particle size distribution affects membrane fouling [26]. A larger particle size results in a lower membrane fouling rate due to the relatively higher settling velocity and the lower probability of particle collisions and attachment to the membrane surface. The particle size distribution of the SNAD granule during different operational phases is shown in Fig. 7. In phase I, particles with a size range of 1.5–2.0 mm accounted for the highest proportion (25%). Particles larger than 2.0 mm and smaller than 1.0 mm accounted for 51% and 10% of all particles, respectively. The particle size had a normal distribution. The average particle size increased with the NaClO concentration in phases II and III, and particles larger than 2.0 mm accounted for 55% and 60%, respectively. These results can be attributed to the increased EPS production that enhanced the SNAD granulation, protecting microorganisms under NaClO stress. Larger SNAD granules typically have better filterability and are more suitable for long-term operations. Thus, the SNAD granule properties contributed to low membrane fouling rates in phases I and II.

However, the average particle size of the SNAD granules decreased as the proportion of particles below 2.5 mm increased. These particles accounted for 48% of all particles in phase IV. The disintegration of the SNAD granules occurred due to bacterial lysis under higher NaClO stress. It should be noted that the SNAD granular structure was significantly affected by the high-concentration NaClO shock in one backwashing cycle, although the backwashing frequency was the lowest (1/30 min), causing prolonged stress of the microorganisms.

3.2.3.2. SMP and EPS

The concentrations of SMP and EPS in the mixed liquor are typically used as membrane fouling indicators [27]. Unlike activated flocs, the SMP in the granular sludge are associated with a decline in the membrane permeability, whereas EPS are related to sludge granulation [28]. The contents and compositions of the SMP and EPS in the SNAD granules in different operational phases were investigated. As shown in Fig. 8a, the SMP_c and SMP_p contents increased from 35.63 and 56.45 mg/L to 45.89 and 80.72 mg/L from phase I to IV, respectively. These results indicated that soluble organic matter was released by the microorganisms under increased NaClO stress. The SMP_p/SMP_c ratio increased from 1.58 to 1.76, suggesting the SMP_p was the main component contributing to the resistance of deep pore blocking. The secondary structure of the protein in the membrane foulants (discussed in Section 3.2.2) suggested that an increase in the NaClO concentration caused the hydrophobicity of the SMP_p, exacerbating membrane fouling and reducing membrane permeability.

In contrast, the EPS trend differed from the SMP trend (Fig. 8b). The EPS_c and EPS_p contents increased from 32.47 and 98.67 mg/g·SS to 39.22 and 127.44 mg/g·SS from phase I to III and then decreased to 38.65 and 120.67 mg/g·SS in phase IV, respectively. The EPS_p/EPS_c ratio showed a similar trend as the EPS contents, with the highest value of 3.25 in phase III. The EPS_p/EPS_c ratio is an indicator of the hydrophobicity and stability of granular sludge [29]. The increments in the EPS contents and EPS_p/EPS_c ratio under NaClO stress indicated suitable sludge granulation and high stability, resulting in high membrane permeability. A decrease in the EPS contents and EPS_p/EPS_c ratio in the later phases was attributed to damage to the bacterial structure under higher NaClO stress, resulting in the disintegration of the SNAD granules and a higher fouling rate.

The components and structures of the SMP and EPS in the SNAD granules were characterized by 3D-EEM fluorescence. As shown in Fig. 9, one fluorescent peak (peak A) was observed at excitation/emission (Ex/Em) wavelengths of 270–280/330–350 nm in phase I. This peak was associated

Table 4
Relative abundance of secondary structures of proteins in membrane foulants during different operational phases

Period	Aggregated strands (1,610~1,625 cm^{-1})/%	α-helix (1,648~1,657 cm^{-1})/%	β-sheet (1,630~1,640 cm^{-1})/%	Random coil (1,640~1,645 cm^{-1})/%	α-helix/ (β-sheet + random coil)
I	11.78	25.08	12.80	13.60	0.950
II	8.80	27.23	13.69	15.26	0.940
III	9.21	25.00	13.17	13.75	0.929
IV	7.36	24.48	13.16	13.51	0.918

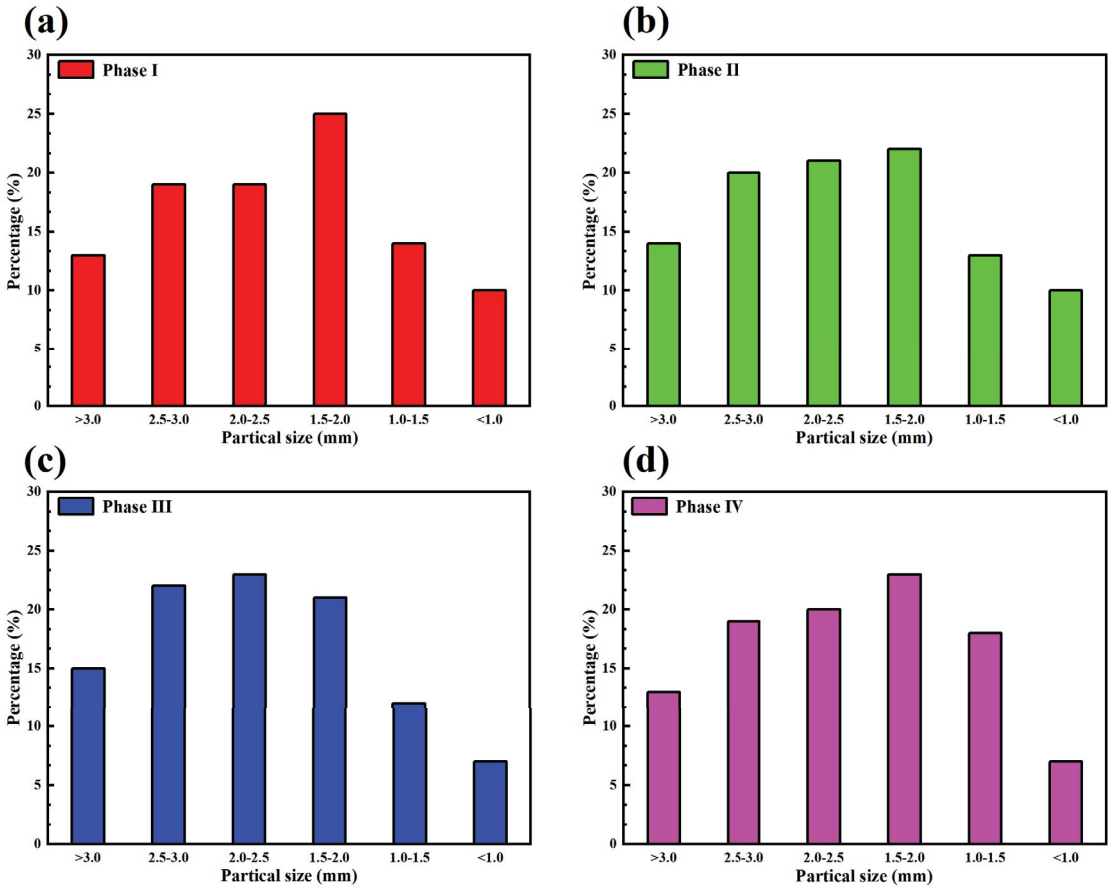

Fig. 7. Change of particle size distribution of SNAD granules during different operational phases.

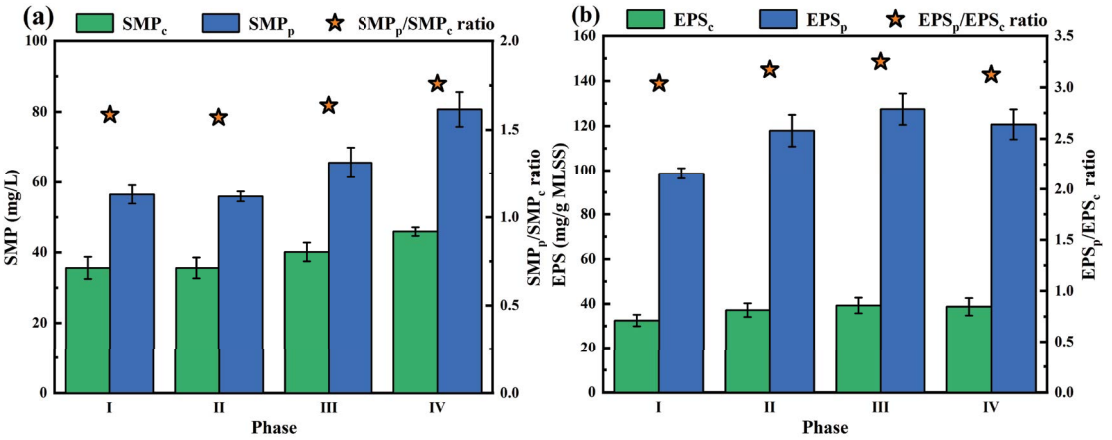

Fig. 8. Changes of (a) SMP and (b) EPS of SNAD granules during different operational phases.

with tryptophan protein-like substances. Another peak (peak B) occurred at Ex/Em wavelengths of 350–360/430–440 nm in phase II–IV; it was attributed to humic acid-like substances. This finding suggested the formation of different components of the protein fraction of SMP after the SNAD granules were exposed to NaClO. In contrast, only one fluorescent peak (peak A) was identified in the EPS fluorescence spectra throughout the test. The fluorescence parameters of SMP and EPS in the SNAD granules, including the peak location, maximum fluorescence intensity, and peak intensity ratios, are summarized in Table 5. The intensities of peaks A and B in the SMP fluorescence spectra increased from phase I to IV, in agreement with the SMP_p contents. Moreover, tryptophan protein-like substances were of critical importance in membrane fouling. However, the intensity of peak A in the EPS fluorescence spectra increased from

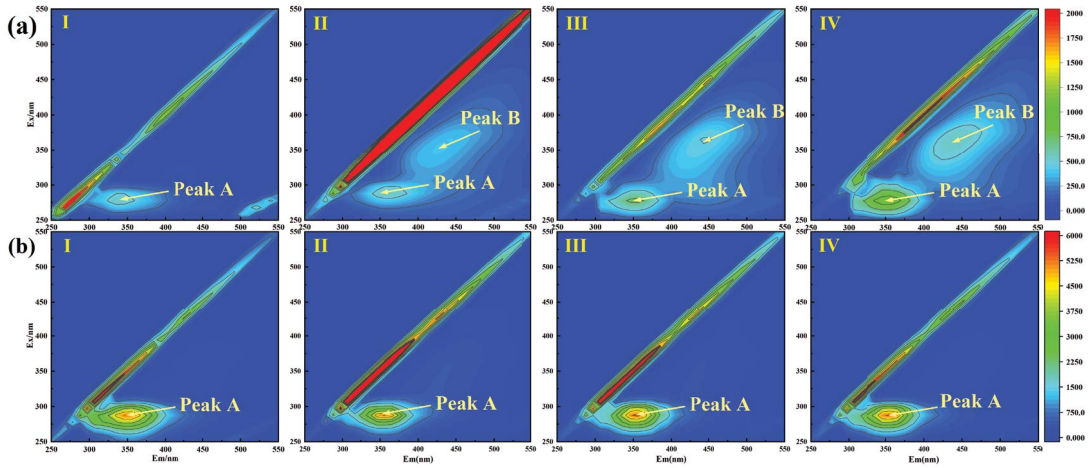

Fig. 9. Three-dimensional fluorescence spectra of (a) SMP and (b) EPS of SNAD granules during different operational phases.

Table 5
Fluorescence spectra parameters of (a) SMP and (b) EPS of the SNAD granules during different operational phases

Sample		Peak A		Peak B		Peak intensity ratio
		Ex/Em	Intensity	Ex/Em	Intensity	A/B
I	SMP	270/330	441.4	–	–	–
	EPS	280/350	5,215	–	–	–
II	SMP	280/350	567.2	350/430	384.9	1.474
	EPS	280/350	5,284	–	–	–
III	SMP	270/350	777.6	360/440	472.2	1.647
	EPS	280/350	5,443	–	–	–
IV	SMP	270/350	1,166.4	360/440	560.9	2.080
	EPS	280/350	5,338	–	–	–

phase I to phase III and then decreased to phase IV, indicating the vital role of tryptophan protein-like substances in maintaining the stability of the SNAD granules.

The NaClO backwashing significantly influenced the metabolic products of the SNAD granules. The SMP and EPS affected the fouling potential of the SNAD granules and membrane fouling.

3.3. Results of redundancy analysis

The relationship between the NaClO concentration/backwashing frequency and the process performance, activities of functional bacteria, and physico-chemical properties of the SNAD granules was assessed using redundancy analysis (Fig. 10). The red arrows represent the NaClO concentration/backwashing frequency, and the green arrows represent the other parameters. An angle between the two arrows smaller than 90° indicates a positive correlation, and an angle greater than 90° indicates a negative correlation [30]. The NaClO concentration had a positive impact on the SMP production but negatively affected the activities of the functional bacteria and the process performance. However, the backwashing frequency exhibited the opposite relationship with these parameters. The reason is the

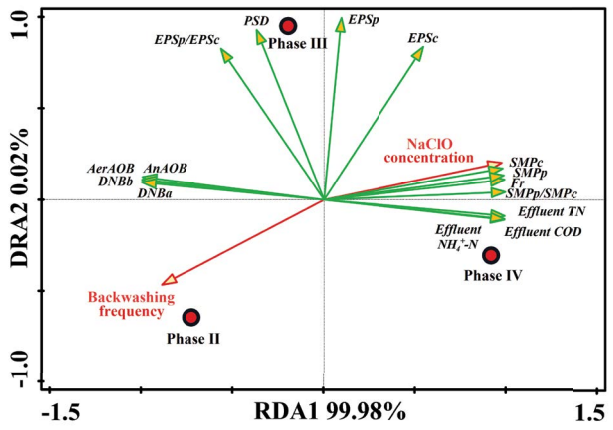

Fig. 10. Redundancy analysis of NaClO backwashing, process performance, activities of functional bacteria and physico-chemical properties of SNAD granules.

contrary trends of the NaClO concentration and the backwashing frequency in one chemical cleaning cycle. NaClO backwashing significantly impacted the biological performance and the fouling potential of the SNAD granules.

An appropriate strategy of periodic NaClO backwashing should be selected to maintain high biological efficacy and membrane permeability in the SNAD-MBR process.

4. Conclusion

This study provided new insights into the influence of *in-situ* NaClO backwashing on the biological performance and membrane fouling behavior in the SNAD-MBR. The biological performance depended on the NaClO concentration and backwashing frequency due to the inhibitory activities of functional bacteria. However, the contribution ratio of the autotrophic and heterotrophic pathways for nitrogen removal remained constant, and the anammox process was dominant throughout the operation. The double-side effects of *in-situ* NaClO backwashing on membrane fouling were elucidated. A lower concentration with a higher frequency provided superior membrane cleaning efficiency, whereas a higher concentration with a lower frequency exacerbated membrane fouling owing to the excessive production of soluble tryptophan protein-like substances. The optimal *in-situ* NaClO backwashing strategy was a NaClO concentration of 10 mg/g·MLSS and a frequency of 1/20 min. This approach can be implemented to broaden the application of the SNAD-MBR process.

Acknowledgements

This work was financially supported by Hebei Natural Science Foundation (E2016402017) and Science and Technology Project of Hebei Education Department (BJ2019029).

References

[1] Z.M. Zheng, S. Huang, W. Bian, D.B. Liang, X.J. Wang, K. Zhang, X.T. Ma, J. Li, Enhanced nitrogen removal of the simultaneous partial nitrification, anammox and denitrification (SNAD) biofilm reactor for treating mainstream wastewater under low dissolved oxygen (DO) concentration, Bioresour. Technol., 283 (2019) 213–220.

[2] B.Y. Li, Y.X. Song, C.H. Liu, Y.Q. He, B. Ma, Rapid cultivation of anammox bacteria by forming free cells in a membrane bioreactor, Water Environ. Res., 93 (2021) 1640–1650.

[3] C.Q. Zhao, G. Wang, X.C. Xu, Y.S. Yang, F.L. Yang, Long-term operation of oxygen-limiting membrane bioreactor (MBR) for the development of simultaneous partial nitrification, anammox and denitrification (SNAD) process, Environ. Technol., 39 (2018) 2193–2202.

[4] Z.W. Wang, J.X. Ma, C.Y.Y. Tang, K. Kimura, Q.Y. Wang, X.M. Han, Membrane cleaning in membrane bioreactors: a review, J. Membr. Sci., 468 (2014) 276–307.

[5] X.M. Han, Z.W. Wang, X.Y. Wang, X. Zheng, J.X. Ma, Z.C. Wu, Microbial responses to membrane cleaning using sodium hypochlorite in membrane bioreactors: cell integrity, key enzymes and intracellular reactive oxygen species, Water Res., 88 (2016) 293–300.

[6] X.M. Han, Z.W. Wang, M. Chen, X.R. Zhang, C.Y.Y. Tang, Z.C. Wu, Acute responses of microorganisms from membrane bioreactors in the presence of NaOCl: protective mechanisms of extracellular polymeric substances, Environ. Sci. Technol., 51 (2017) 3233–3241.

[7] W.W. Cai, Y. Liu, Enhanced membrane biofouling potential by on-line chemical cleaning in membrane bioreactor, J. Membr. Sci., 511 (2016) 84–91.

[8] X.D. Yue, Y.K.K. Koh, H.Y. Ng, Membrane fouling mitigation by NaClO-assisted backwash in anaerobic ceramic membrane bioreactors for the treatment of domestic wastewater, Bioresour. Technol., 268 (2018) 622–632.

[9] Z.Z. Wang, F.G. Meng, X. He, Z.B. Zhou, L.N. Huang, S. Liang, Optimisation and performance of NaClO-assisted maintenance cleaning for fouling control in membrane bioreactors, Water Res., 53 (2014) 1–11.

[10] C.K. Jiang, X. Tang, H. Tan, F. Feng, Z.M. Xu, Q. Mahmood, W.Z. Zeng, X.B. Min, C.J. Tang, Effect of scrubbing by NaClO backwashing on membrane fouling in anammox MBR, Sci. Total Environ., 670 (2019) 149–157.

[11] American Public Health Association (APHA), American Water Works Association (AWWA), Water Environment Federation (AEF), Standard Methods for the Examination of Water and Wastewater, American Public Health Association (APHA), Washington, D.C., USA, 2005.

[12] X.Y. Li, S.F. Yang, Influence of loosely bound extracellular polymeric substances (EPS) on the flocculation, sedimentation and dewaterability of activated sludge, Water Res., 41 (2007) 1022–1030.

[13] J. Wu, H.M. Zhou, H.Z. Li, P.C. Zhang, J. Jiang, Impacts of hydrodynamic shear force on nucleation of flocculent sludge in anaerobic reactor, Water Res., 43 (2009) 3029–3036.

[14] Z.Z. Wang, P. Gao, L. Yan, D. Zhao, Y. Ji, H. Zhang, S.M. Li, Simultaneous nitritation, anammox, and denitrification (SNAD) process in a membrane bioreactor: start-up, optimization, and membrane fouling behavior, Desal. Water Treat., 194 (2020) 69–84.

[15] W.G. Wang, Y. Yan, Y.H. Zhao, Q. Shi, Y.Y. Wang, Characterization of stratified EPS and their role in the initial adhesion of anammox consortia, Water Res., 169 (2020) 115223, doi: 10.1016/j.watres.2019.115223.

[16] S. L. de Sousa Rollemberg, A.N. de Barros, V.N.S.A. Lira, P.I.M. Firmino, A.B. dos Santos, Comparison of the dynamics, biokinetics and microbial diversity between activated sludge flocs and aerobic granular sludge, Bioresour. Technol., 294 (2019) 122106, doi: 10.1016/j.biortech.2019.122106.

[17] H. Chen, S. Liu, F. Yang, Y. Xue, T. Wang, The development of simultaneous partial nitrification, anammox and denitrification (SNAD) process in a single reactor for nitrogen removal, Bioresour. Technol., 100 (2009) 1548–1554.

[18] F.R. Cai, L.R. Lei, Y.M. Li, Y.C. Chen, A review of aerobic granular sludge (AGS) treating recalcitrant wastewater: refractory organics removal mechanism, application and prospect, Sci. Total Environ., 782 (2021) 146852, doi: 10.1016/j.scitotenv.2021.146852.

[19] E.J. Lee, J.S. Kwon, H.S. Park, W.H. Ji, H.S. Kim, A. Jang, Influence of sodium hypochlorite used for chemical enhanced backwashing on biophysical treatment in MBR, Desalination, 316 (2013) 104–109.

[20] T. Kurita, K. Kimura, Y. Watanabe, The influence of granular materials on the operation and membrane fouling characteristics of submerged MBRs, J. Membr. Sci., 469 (2014) 292–299.

[21] Z.Z. Wang, Y. Ji, L. Yan, Y. Yong, H. Zhang, P. Gao, S.M. Li, Simultaneous anammox and denitrification process shifted from the anammox process in response to C/N ratios: performance, sludge granulation, and microbial community, J. Biosci. Bioeng., 130 (2020) 319–326.

[22] Z.W. Wang, Z.C. Wu, S.J. Tang, Extracellular polymeric substances (EPS) properties and their effects on membrane fouling in a submerged membrane bioreactor, Water Res., 43 (2009) 2504–2512.

[23] K. Zhang, J. Zhang, J. Li, Z.M. Zheng, M.X. Sun, Analyzing the roles of cyclic dimeric guanosine monophosphate (c-di-GMP) on the formation of autotrophic granules and autotrophic biofilm in integrated fixed-film activated sludge (IFAS) reactor, Environ. Technol. Innovation, 26 (2022) 102304, doi: 10.1016/j.eti.2022.102304.

[24] O.T. Iorhemen, R.A. Hamza, M.S. Zaghloul, J.H. Tay, Aerobic granular sludge membrane bioreactor (AGMBR): extracellular

polymeric substances (EPS) analysis, Water Res., 156 (2019) 305–314.
[25] F.X. Jia, Q. Yang, X.L. Liu, Y.Z. Peng, B.K. Li, L. Zhang, Y.Z. Peng, Stratification of extracellular polymeric substances (EPS) for aggregated anammox microorganisms, Environ. Sci. Technol., 51 (2017) 3260–3268.
[26] W.X. Zhang, F. Jiang, Membrane fouling in aerobic granular sludge (AGS)-membrane bioreactor (MBR): effect of AGS size, Water Res., 157 (2019) 445–453.
[27] O.T. Iorhemen, R.A. Hamza, J.H. Tay, Membrane fouling control in membrane bioreactors (MBRs) using granular materials, Bioresour. Technol., 240 (2017) 9–24.
[28] O.T. Iorhemen, R.A. Hamza, J.H. Tay, Membrane bioreactor (MBR) technology for wastewater treatment and reclamation: membrane fouling, Membranes, 6 (2016) 33, doi: 10.3390/membranes6020033.
[29] F. Anjum, I.M. Khan, J.H. Kim, M.H. Aslam, G. Blandin, M. Heran, G. Lesage, Trends and progress in AnMBR for domestic wastewater treatment and their impacts on process efficiency and membrane fouling, Environ. Sci. Technol., 21 (2021) 101204, doi: 10.1016/j.eti.2020.101204.
[30] A. Ding, L. Quan, X. Guo, H.Q. Wang, Y.Y. Wen, J. Liu, L.L. Zhang, D.J. Zhang, P.L. Lu, Storage strategy for shale gas flowback water based on non-bactericide microorganism control, Sci. Total Environ., 798 (2021) 149187, doi: 10.1016/j.scitotenv.2021.149187.